

Article

# Real Time Scheduling of a Microgrid Equipped with Ultra-Fast Charging Stations

Luigi Pio di Noia , Fabio Mottola , Daniela Proto \* and Renato Rizzo

Department of Electrical Engineering and Information Technology, University of Naples Federico II, 80125 Naples, Italy; luigipio.dinoia@unina.it (L.P.d.N.); fabio.mottola@unina.it (F.M.); renato.rizzo@unina.it (R.R.)  
\* Correspondence: daniela.proto@unina.it

**Abstract:** Ultra-fast charging infrastructures are gaining increasing interest thanks to their ability to reduce the charging-time of plug-in electric vehicles to values comparable to those of the refueling of traditional vehicles in gas stations. This is a consequence of the increasing rated power of both on-board batteries and charging equipment. On the other hand, the increased values of charging power have led to an increased impact on the power distribution networks, particularly in terms of line currents and bus voltages. In presence of large penetration of ultra-fast charging devices, in fact, both currents and voltages are affected by larger variations whose values can exceed the admissible limits imposed by the technical constraints and by the levels of quality of service. In order to reduce the impact of this typology of vehicles' charging on the electrical infrastructure, in this paper a methodology is presented which allows managing a microgrid in presence of ultra-fast charging stations by satisfying the constraints of the grid, while preserving the expected short charging-time for electric vehicles. To this end, a proper optimal strategy is proposed which coordinates the demands of electric vehicles and of the other loads of the microgrid with the power provided by the renewable energy generation resources. The proposed approach aims to optimally control the active and reactive power of charging stations and renewable generation units and to minimize the charging time of a fleet of plug-in electric vehicles while satisfying the constraints on the technical aspects and on the quality of service. The proposed approach has been tested on a test system and the results, proposed in the last part of the paper, demonstrate the feasibility of the proposed approach.

**Keywords:** ultra-fast charging station; extreme fast charging; plug-in electric vehicle; microgrid; real-time scheduling; optimal scheduling



**Citation:** di Noia, L.P.; Mottola, F.; Proto, D.; Rizzo, R. Real Time Scheduling of a Microgrid Equipped with Ultra-Fast Charging Stations. *Energies* **2022**, *15*, 816. <https://doi.org/10.3390/en15030816>

Academic Editor: Wiseman Yair

Received: 6 December 2021

Accepted: 20 January 2022

Published: 23 January 2022

**Publisher's Note:** MDPI stays neutral with regard to jurisdictional claims in published maps and institutional affiliations.



**Copyright:** © 2022 by the authors. Licensee MDPI, Basel, Switzerland. This article is an open access article distributed under the terms and conditions of the Creative Commons Attribution (CC BY) license (<https://creativecommons.org/licenses/by/4.0/>).

## 1. Introduction

Thanks to their ability to provide a refueling capability similar to that of traditional combustion engine vehicles, ultra-fast charging (UFC) infrastructures for plug-in electric vehicles (PEVs) are gaining particular interest from researchers.

UFC stations imply DC charging that is, the AC power delivered from the grid is converted into DC by means of the off-board converter included in the charging station. Compared to AC charging stations that require onboard vehicle converters, the DC allows more power charging, up to 350 kW, and faster charging, a full charge in less than 15 min. This technology, however, is brand new and there are still several challenges to meet.

Due to the large power requirement, a UFC station connected to medium voltage networks allows reducing losses by about 75% compared to those due to a charger of the same power rating connected to the low voltage grids [1,2]. The chargers can be installed as single- or multiple stall units and include three-phase AC/DC rectification stages supplied by a dedicated transformer.

With reference to the architecture, UFC stations can have a common AC or a common DC bus. In an AC bus configuration, the transformer individually supplies the charging columns, and each charging unit has its own rectification stage connected to the AC bus. In

the DC bus configuration, the transformer supplies power to a low voltage rectifier, which provides the DC power to the standalone sub-stations [2,3]. In addition, with reference to the DC bus configuration, UFCs can have a unipolar or bipolar voltage bus, being in both the cases the AC-DC stage common to all the PEVs [4]. As discussed in [5] ultrafast methods aim at charging electric vehicles in a time comparable to that of gas refueling. In [6] the setup of a charging station, having these capabilities is also discussed. Recently, both electric vehicles and charger devices have been made commercially available.

With reference to the charging technique, common approaches are the constant current–constant voltage (CC–CV) and the five-step charging pattern, both aimed at prolonging the battery lifecycle. The former is based on a constant current charging process until a certain voltage value is reached. After that, the battery is charged at a constant voltage rate. The latter technique distributes the charging time into five steps each characterized by a different constant current value with voltage increasing during the step. Pre-set limit voltage values at each step determine the new charging current, that is the following step [4,7].

Regarding the control strategy of PEV charging stations, a number of studies have been proposed in the technical literature. Comprehensive reviews of the proposed strategies can be found in [8,9]. The review in [8] envisages the control strategies based on three control levels of the aggregator. The Level-1 is referred to as the substation level, the Level-2 is the feeder level, and Level-3 refers to the microgrid level aggregators. More specifically, it proposes a review of the recent literature related to this multilevel control of PEVs integrated with distributed generators in a microgrid system. A study of a global controller to achieve coordination between multi-level aggregators is also proposed. The review in [9] proposes a review of PEVs' optimal charging and scheduling under dynamic pricing schemes and discusses the two charging frameworks available in the smart grid environment, i.e., centralized and decentralized. In the review it is inferred that the main optimization methods employed in a dynamic pricing environment are aimed to achieve objectives such as electricity cost minimization [10–12], peak load reduction [13], power loss reduction and voltage regulation [14,15], distribution lines overloading minimization [16], and the combination of multiple grid services [17]. In [18] a power flow analysis is performed to study the impact of PEVs charging on network bus voltages. In [19] an online procedure is proposed for scheduling the charging of electric vehicles aimed at flattening solar “duck curves”, which includes a combination of a heuristic function and a neural network.

All of the aforementioned studies tend to focus on the services to be provided to the grid and/or on the impact the vehicles' charging has on the grid [2,20]. On the other hand, the vehicle's charging speed is a crucial issue in the case of UFC which needs to be maximized while considering technical constraints of the grid. The aim of this paper is to propose a real-time scheduling of microgrids including UFC stations and renewable-based distributed generation (DG) units. The proposed approach exploits a constrained optimal power flow (OPF)-based method which performs a predictive load flow scheduling based on a very short-time forecast of not-dispatchable loads and resources aimed at maximizing the power for charging purposes (so minimizing the charging time of the vehicles). The optimization is carried out by satisfying the technical constraints of the grids thanks to the optimal management of the maximum power available for the UFC stations and controlling the reactive power made available by the converter-interfaced resources (UFC stations and DG units). It is worth noting that the proposed procedure does not consider frequency control which could be an important issue in the case of island mode operating conditions and high power requests from PEVs [21].

The main contributions of this paper are summarized as follows:

- an optimal power flow is proposed which includes ultrafast charging stations in terms of active and reactive power provision;
- the optimal power flow takes into consideration actual models of PEVs' charging strategies;
- renewable-based distributed generation units are coordinated with loads and charging stations for the optimal balance of both active and reactive powers;

- the proposed management approach is aimed at minimizing the charging time of the vehicles, avoiding curtailment of the power available to the charging stations, and preserving power quality and secure operation of the network;
- the real-time procedure allows repeated updating of the schedule of active and reactive power of different resources based on the current conditions.

From a practical point of view, this paper provides a tool able to guarantee massive penetration of PEVs with fast charging requirements through optimal integration of UFC stations in distribution grids whose wide diffusion is expected in the next future. The scientific contribution of the paper resides on the proposal of a novel methodological approach which includes the formulation of a proper optimization problem. To the best of the authors' knowledge, none of the papers proposed in the current technical literature has treated the problem of UFC stations in such a comprehensive way considering the network requirements in terms of power quality issues, the vehicles' requirement in terms of charging speed, and the changing conditions of renewable generation availability and load request.

The remainder of the paper is organized as follows: Section 2 describes the proposed scheduling strategy; Section 3 shows the results of numerical applications; conclusions are drawn in Section 4.

## 2. The Proposed Real-Time Scheduling Strategy

The proposed strategy refers to the real-time scheduling of microgrids in presence of UFC stations and renewable-based DG units. Fast charging is typically referred to as Level 3, which is characterized by charging equipment of 480 AC or 600 DC supplying systems, with a maximum power up to 43.5 kW and 200 kW, respectively [5]. UFC methods refer to even higher power supplied at DC supplying systems with voltage levels of 800 kV or higher and power of 350 kW or higher. Due to the reduced time of these fast-charging architectures (about ten minutes), the real-time scheduling requires optimization approaches performed with respect to controlled time intervals lower than those usually adopted in the energy management [22].

The proposed approach exploits a constrained OPF-based method which performs a predictive load flow scheduling based on very short-time forecast of not-dispatchable loads and resources. The approach is aimed at controlling the power available for charging purposes and the reactive power made available by the converter-interfaced resources for grid support purposes. More specifically, the goal of the proposed strategy is the minimization of the charging time of PEVs, the objective function being defined as the sum of the powers provided to all the electric vehicles connected to the charging stations. This function is maximized, so allowing a reduction in the charging time. Constraints are imposed on the technical limitation of the charging devices and of the microgrid as well as limitations related to the quality of service.

The UFC station is assumed to be directly connected to an MV microgrid through an AC/DC power converter interface. UFC stations are made by several chargers, each equipped with a DC/DC fast-charging device, according to the DC-coupled architecture. This solution includes solid state transformer technology, whose recent improvements allow enhanced power density and efficiency of the fast-charging infrastructures [5]. A scheme of the considered configuration is shown in Figure 1, where  $n$  positions (i.e., single stall units) for the PEVs' chargers are considered. A local renewable-based generation and a storage device can be also included in the infrastructure of the UFC station.

In particular, inputs of the procedure include offline and online information. The offline inputs, which can be changed offline if modifications occur, are the line ampacities, admissible bus voltage ranges, transformer rating, the capability curve of the DG units, and the location and rating of the UFC stations connected to the microgrid. Online inputs are those that must be updated at each time interval, they include: the forecast of the active and reactive load demand and of the power produced by the DG units, as well as the number

and location of the PEVs connected to the UFC stations, together with their required SoC at departure and the initial SoC at the considered time interval.

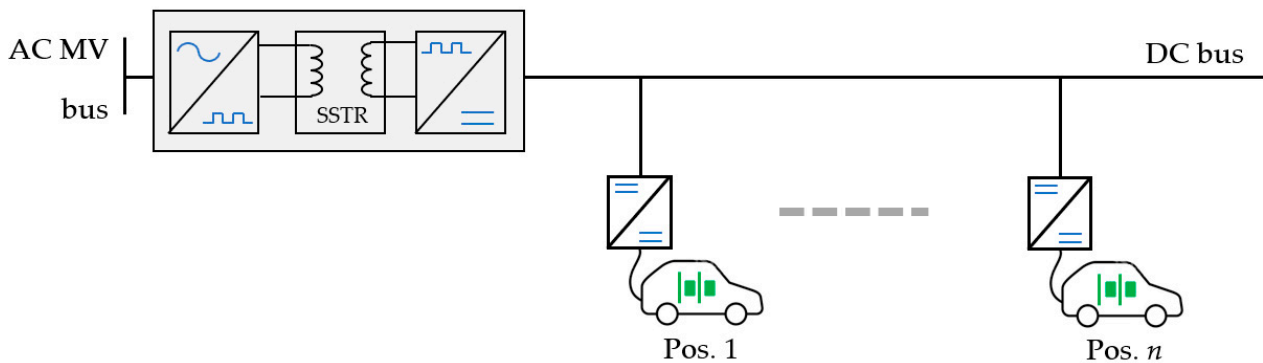


Figure 1. Scheme of the UFC station connected to an MV network.

The considered DG units are those typically included in modern electrical systems, based on renewable energy sources, such as wind or solar energy, connected to the micro-grid through power converters able to control the reactive power.

The proposed strategy is performed at each time interval of the day with respect to the inputs and outputs summarized in Figure 2.

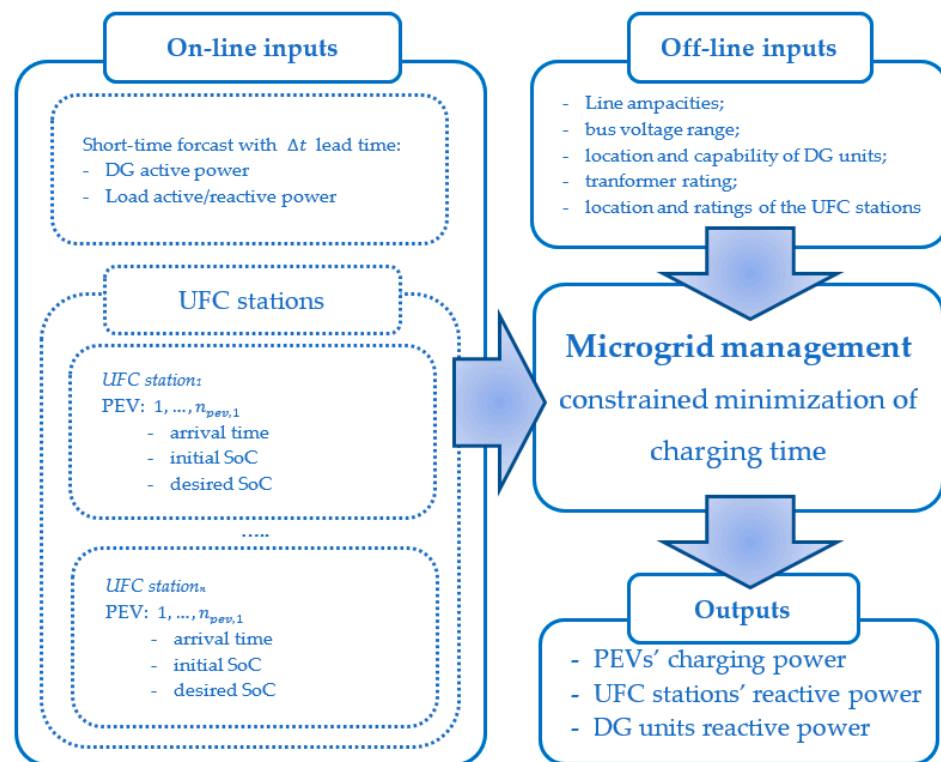


Figure 2. Flow chart scheme of the proposed real-time scheduling strategy.

The proposed scheduling strategy is formulated according to a constrained minimization problem aimed at allowing fast charging while satisfying the microgrid constraints. Optimization variables are the active power requested by each PEV, the reactive power provided by the UFC stations and the DG units, and the magnitude and argument of voltage at each busbar of the microgrid. In the following sub-sections, the objective function and the equality and inequality constraints are presented in detail.

### 2.1. Objective Function

The objective function to maximize is the power that the microgrid provides to the UFC stations to charge PEVs, that is:

$$f_{obj,k} = \sum_{j=1}^{n_{cs}} \sum_{i=1}^{n_{pev,j,k}} P_{pev,i,j,k}, \quad (1)$$

where  $n_{cs}$  is the number of the UFC stations connected to the microgrid,  $n_{pev,j,k}$  is the number of PEVs connected at the  $j$ th charger at the time interval  $k$ , and  $P_{pev,i,j,k}$  is the charging power of the  $i$ th PEV connected to the  $j$ th UFC station at the  $k$ th time interval.

### 2.2. Constraints on the Plug-In Vehicles' Fleets

The constraints imposed on the charging powers of the PEVs depend on the limitations imposed by both UFC stations and on-board batteries of the PEVs.

The active and reactive powers that UFC stations can request of the grid are then subject to the following constraints:

$$\sum_{i=1}^{n_{pev,i,k}} P_{pev,i,j,k} \leq P_{cs,j}^n \quad (2)$$

$$\sqrt{\left(\sum_{i=1}^{n_{pev,i,k}} P_{pev,i,j,k}\right)^2 + Q_{cs,j,k}^2} \leq S_{cs,j}^n \quad (3)$$

$$j = 1, \dots, n_{cs}$$

where  $P_{cs,j}^n$  is the installed power of the  $j$ th UFC station,  $Q_{cs,j,k}$  is the reactive power of the  $j$ th UFC station at the time interval  $k$ , and  $S_{cs,j}^n$  is the nominal power of the AC/DC converter of the  $j$ th UFC station.

By focusing on each charger, the charging power can exceed neither the charger rating nor the power allowed by the connected on-board battery, that is:

$$P_{pev,i,j,k} \leq \min\{P_{pev,i,j}^n, P_{SoC,i,j,k}^{max}\} \quad (4)$$

$$i = 1, \dots, n_{pev,j,k}, \quad j = 1, \dots, n_{cs}$$

where  $P_{pev,i,j}^n$  is the power rating of the  $i$ th charger of the  $j$ th UFC station, and  $P_{SoC,i,j,k}^{max}$  the maximum charging power of the on-board battery connected to the  $i$ th charger of the  $j$ th UFC station. Typical charging procedures of the batteries are based on two stages: the first is performed at lower values of SoC (typically,  $SoC < 0.8$ ) and refers to the charging stage at constant current; the second, performed at higher SoC levels, refers to the charging stage at constant voltage [23]. The power corresponding to these stages,  $P_{SoC,i,j,k}^{max}$  is then typically approximated by:

$$P_{SoC,i,j,k}^{max} = \begin{cases} P_{SoC,i,j,k}^n & \text{if } SoC_{i,j,k-1} < 0.8 \\ P_{pev,i,j}^n e^{-\lambda_{i,j}(SoC_{i,j,k-1}-0.8)} & \text{if } SoC_{i,j,k-1} \geq 0.8 \end{cases} \quad (5)$$

$$i = 1, \dots, n_{pev,j,k}, \quad j = 1, \dots, n_{cs}$$

where  $P_{SoC,i,j,k}^n$  is the power rating of the onboard battery. The decay constant  $\lambda_{i,j}$  is defined according to a control law which must fit a compromise between charge velocity and battery lifetime preservation.

In Equation (6) where the value of  $SoC_{i,j,k}$  depends on the charging power provided to the PEV during the charging stage, then it is given by:

$$SoC_{i,j,k} = SoC_{i,j,k-1} + \frac{1}{E_{pev,i,j}^n} \eta_{pev,j} P_{pev,i,j,k} \Delta t, \quad (6)$$

$$i = 1, \dots, n_{pev,j,k}, \quad j = 1, \dots, n_{cs}$$

where  $E_{pev,i,j}^n$  is the on-board battery capacity of the PEV connected to the  $i$ th charger of the  $j$ th UFC station,  $P_{pev,i,j,k}$  is the charging power of the  $i$ th charger of the  $j$ th UFC station at the time interval  $k$ ,  $\eta_{pev,j}$  is the efficiency of the chargers located at the  $j$ th UFC station, and  $SoC_{i,j,k-1} = SoC_{i,j,0}$  when  $k$  is the interval corresponding to the arrival time of the PEV, i.e., a specified input value of SoC,  $SoC_{i,j,0}$  is known at the beginning of the charging stage of each PEV. When the SoC of each vehicle reaches the desired value at the departure time,  $SoC_{dp,i,j}$ :

$$SoC_{i,j,k} = SoC_{dp,i,j}. \quad (7)$$

$$i = 1, \dots, n_{pev,j,k}, \quad j = 1, \dots, n_{cs}$$

The PEV's battery connected to the  $i$ th charger of the  $j$ th UFC station is assumed fully charged and the UFC station is available to receive another PEV.

### 2.3. Constraints on the Microgrid Buses

With reference to the whole microgrid, the constraints are those typically included in the optimal power flow analyses. It is assumed that the microgrid is connected to the upstream grid through a point of common coupling (PCC).

Equality constraints are imposed on the active and reactive power balance at all buses of the network in terms of load flow equations:

$$P_{i,k} = V_{i,k} \sum_{j=1}^n V_{j,k} \left[ G_{i,j} \cos(\delta_{i,k} - \delta_{j,k}) + B_{i,j} \sin(\delta_{i,k} - \delta_{j,k}) \right] \quad (8)$$

$$Q_{i,k} = V_{i,k} \sum_{j=1}^n V_{j,k} \left[ G_{i,j} \sin(\delta_{i,k} - \delta_{j,k}) - B_{i,j} \cos(\delta_{i,k} - \delta_{j,k}) \right] \quad (9)$$

$$i = 1, \dots, n$$

where, with reference to the time interval  $k$ ,  $P_{i,k}$  ( $Q_{i,k}$ ) is the active (reactive) power injected into the bus  $i$ ,  $V_{i,k}$  ( $\delta_{i,k}$ ) and  $V_{j,k}$  ( $\delta_{j,k}$ ) are the magnitudes (arguments) of the voltage at the buses  $i$  and  $j$ , respectively,  $G_{i,j}$  and  $B_{i,j}$  are the real and imaginary parts of the network admittance matrix, and  $n$  is the number of network buses. The bus #1 of the network is assumed to be the slack bus, thus further equality constraints are imposed on the magnitude and argument of the bus voltage at the generic time interval  $k$ :

$$V_{1,k} = V_1^{sp} \quad (10)$$

$$\delta_{1,k} = 0 \quad (11)$$

The injected active and reactive power at the left side of the load flow of Equations (8) and (9), ( $P_{i,k}$  and  $Q_{i,k}$ ), can include specified values related to load active and reactive powers and active power provided by renewable energy sources, all derived from short-term forecast. The optimization variables regarding the active power of PEVs' chargers and the reactive power provided by both UFC stations and DG units are also included.

The inequality constraints refer to the bus voltage, which cannot exceed an admissible range, and to the line currents, which cannot exceed the lines' ampacities:

$$V_{min}^{sp} \leq V_{i,k} \leq V_{max}^{sp} \quad (12)$$

$$\begin{aligned}
 i &= 1, \dots, n \\
 I_{l,k} &\leq I_l^{rtd} \\
 l &\in \Omega_l
 \end{aligned} \tag{13}$$

where  $V_{min}^{sp}$  ( $V_{max}^{sp}$ ) is the minimum (maximum) voltage magnitude allowed at all buses of the microgrid,  $I_{l,k}$  is the line current flowing through the line  $l$ ,  $I_l^{rtd}$  is its ampacity, and  $\Omega_l$  is the set of the lines of the microgrid. Note that the voltages at buses different from the slack bus are implemented in the optimal power flow approach as optimization variables. Trivial relationships can also be derived to express the line currents as a function of the bus voltages and then, of the optimization variables.

An inequality constraint is imposed on the power flowing through the transformers of the microgrid, which cannot exceed their rated power:

$$\begin{aligned}
 \sqrt{P_{i,k}^2 + Q_{i,k}^2} &\leq S_{tr,i}^{rtd} \\
 i &\in \Omega_{TR}
 \end{aligned} \tag{14}$$

where  $\Omega_{TR}$  is the set of transformers included in the microgrid, and  $S_{tr,i}^{rtd}$  is the rated power of the  $i$ th transformer.

A further inequality constraint applies to the apparent power provided by the renewable DG units which cannot exceed the rating of the power converter interface:

$$\begin{aligned}
 \sqrt{P_{i,k}^2 + Q_{i,k}^2} &\leq S_{DG}^{rtd} \\
 i &\in \Omega_{DG}
 \end{aligned} \tag{15}$$

where  $\Omega_{DG}$  is the set of buses where the DG units are connected. In Equation (15), the active power injected into the bus is assumed to be a specified value derived by a short-term forecast; the reactive power is assumed as an optimization variable.

To provide an external service to the upstream network, the UFC stations and the DG systems can be used to provide reactive power support to limit the power factor at the PCC, such that:

$$\cos\left(\tan^{-1}\left(\frac{Q_{PCC,k}}{P_{PCC,k}}\right)\right) \leq \cos\varphi_{max} \tag{16}$$

where  $Q_{PCC,k}$  and  $P_{PCC,k}$  are the reactive and active power imported from the upstream network at the PCC.

### 3. Numerical Simulations

In this Section some results of the application of the proposed real-time procedure are reported with respect to the microgrid schematized in Figure 3, which refers to the 12.47 kV, three-phase, balanced Cigrè benchmark system [24]. It includes two feeders with 15 buses; the two feeders are connected to the upstream network through two 115/12.47 kV transformers of 50 and 20 MVA. Note that, to accommodate a larger load demand, the size of the first transformer has been modified with respect to that of the original benchmark system.

The data of the loads are reported in Table 1. The loads are assumed to vary during the day according to a typical profile [24] as that shown in Figure 4 which refers to the load connected at bus #6. Two photovoltaic (PV) units are connected to the buses #9 and #15, each of 0.5 MW rated power. Figure 5 shows a typical daily profile of the PV connected at bus #9 [25]. Four charging stations are considered connected to the buses #4, #7, #12, and #15. Each UFC station is equipped with four 350 kW-DC/DC extra fast chargers and connected to the microgrid through an AC/DC power converter having a rated power of 1.4 MW. It is assumed, that these converters can be controlled to provide the regulation of the reactive power. The overall efficiency of the charging station is 97% [22].

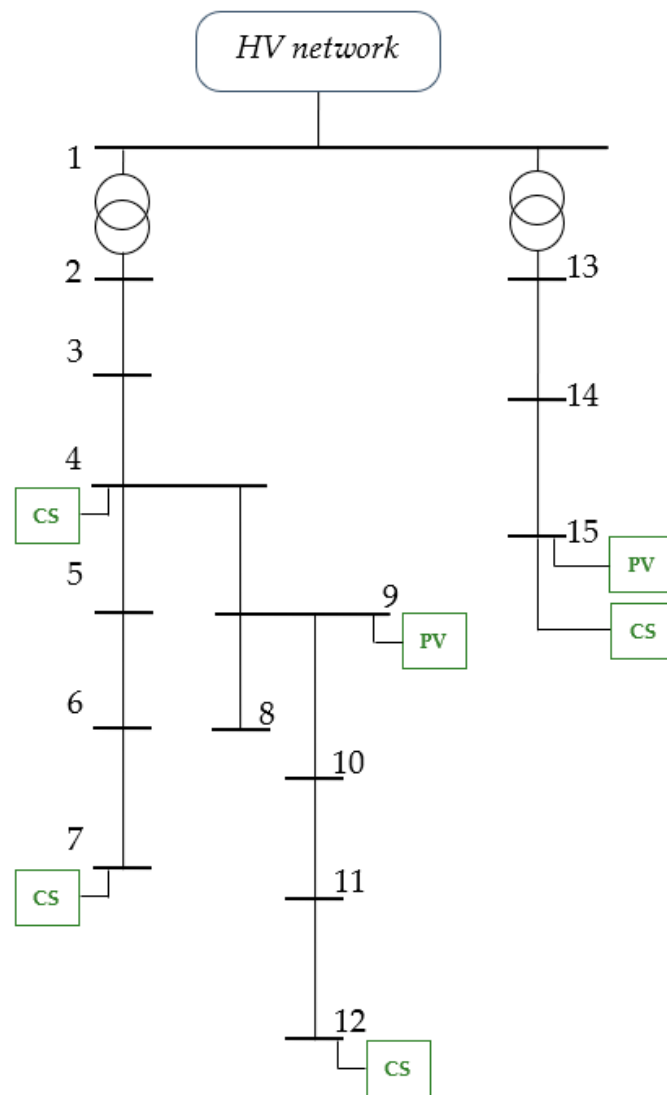
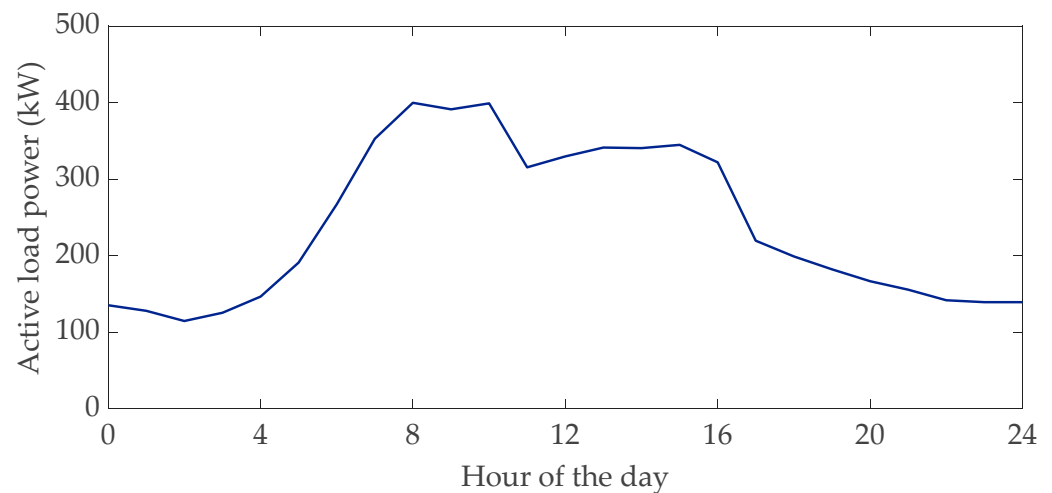


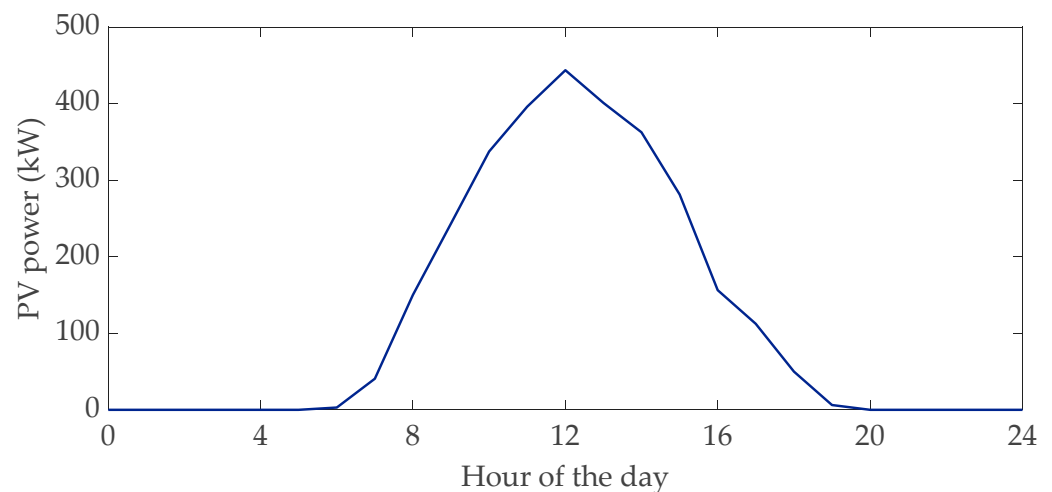
Figure 3. The microgrid under study.

Table 1. Load Input data.

Bus Number	Rated Power (MVA)	$\cos \varphi$	Bus #	Rated Power (MVA)	$\cos \varphi$
2	13.8	0.93	8	0.30	0.95
	9.16	0.87		0.25	0.90
3	0.35	0.95	9	0.20	0.90
	0.80	0.85		0.35	0.95
4	0.25	0.90	11	0.50	0.90
	0.24	0.80		0.10	0.95
5	0.40	0.90	12	0.45	0.85
	0.20	0.95		3.20	0.90
6	0.30	0.85	13	3.78	0.87
	0.15	0.95		0.68	0.85
8	0.10	0.95	15	0.27	0.90



**Figure 4.** Daily profile of the loads connected at bus #6.



**Figure 5.** Daily profile of the PV unit located at bus #9.

The proposed approach has been applied, assumed to be at 11.00 a.m., which corresponds to a time of the day with critical peak load demand (see Figure 4) and considering a time interval duration ( $\Delta t$ ) of one minute. Starting from 11.00 a.m., the arrival of some PEVs has been simulated with 0.2 SoC and requiring 0.9 SoC at the departure. For each vehicle, it is assumed that the arrival time occurs within five minutes from the departure time of the vehicle previously connected to the charger. It is also assumed that it randomly varies according to a uniform distribution. Note that at the beginning of the simulation all chargers are assumed to have no connected vehicles.

During the period of the simulation, the PV power production and load requests are assumed to vary according to a uniform distribution in a range of  $\pm 2\%$  around the corresponding hourly mean value. As an example, Figure 6 reports the power profile of the load at bus #6 related to the considered time.

The battery on board of each plugged-in vehicle has a capacity of 100 kWh, which is a typical size of the battery that can support ultra-fast charging [26]. According to constraints (5), the upper limit of the charging power for this typology of battery depends on the SoC. In this application, the assumed power limit is reported in Figure 7 for different SoC values, this limit being identified according to the requirements of the battery connected to the UFC station in terms of SoC dependence, charging time, and battery lifetime preservation [23]. With reference to a 100 kWh battery with a SoC of 20% at the arrival, about 20 min are required to reach 90% of SoC; if a value of 80% of SoC is desired at the departure, then about 10 min are needed.

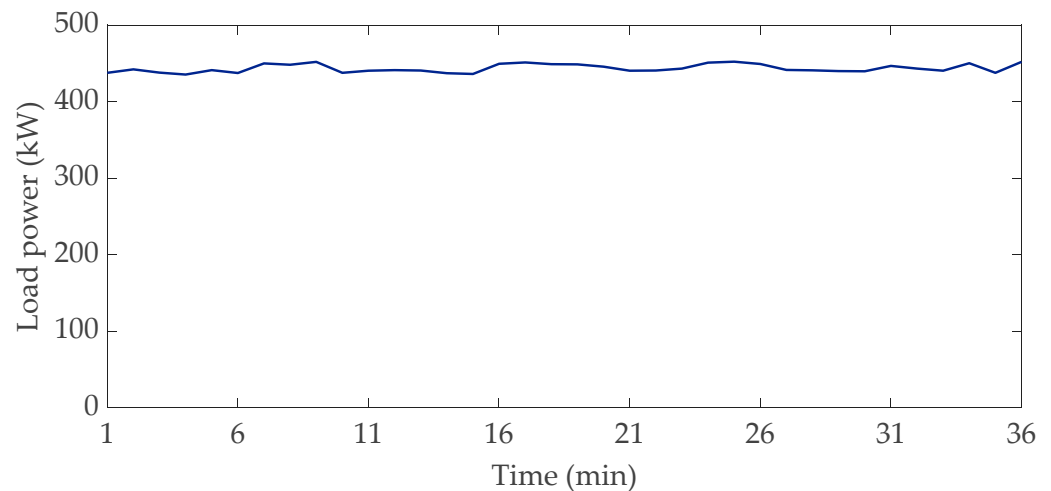


**Figure 6.** Profile of the load at bus #6 during the simulation period.

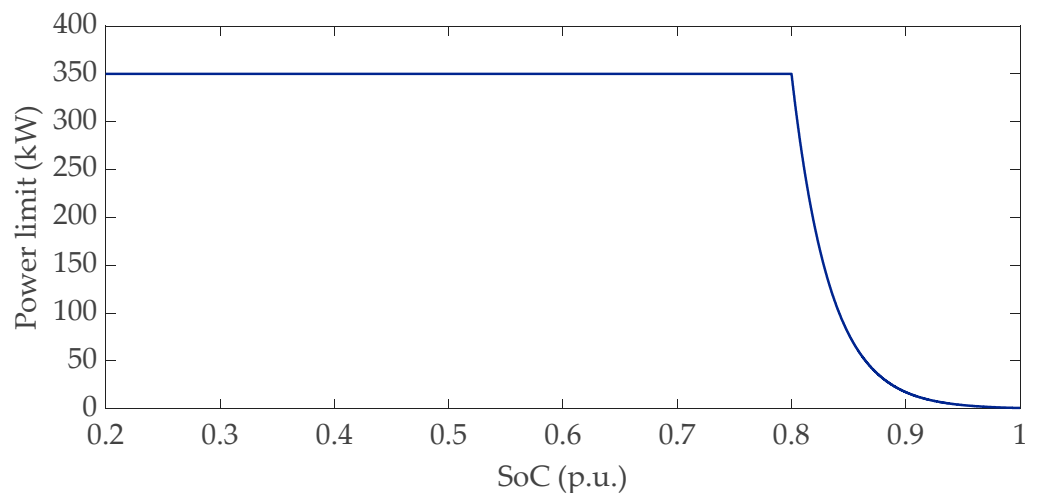


**Figure 7.** Profile of the limit of the charging power related to the SoC.

Next, the results of the application of the proposed approach are reported and compared to those related to the uncontrolled case, which refers to the operation of the microgrid under study with the PEVs charged with the maximum power allowed, according to the curve in Figure 7. Thus, three case studies are considered:

- *case (0)*: uncontrolled PEVs' charge;
- *case (1)*: controlled PEVs' charge;
- *case (2)*: controlled PEVs' charge with reactive power control at the PCC.

The selection of the last two case studies allows evaluation of the impact of the reactive power support of the UFC stations on the fast-charging performances, being the constraint (16) related to the reduction of the power factor at the PCC of the microgrid. In *case (2)*, a maximum power factor of 0.9 is imposed. The results reported in this Section refer to a simulation lasting 36 min. This period has been chosen to allow the simulation of complete charge of a specific number of vehicles that, for comparative purposes, have to be the same in each of the considered case studies.

In Table 2 the arrival time of the PEVs to the chargers of each charging stations are reported.

The results in terms of charging time of each vehicle connected to each charging station are reported in Table 3, together with the arrival time. Note that only the vehicle whose charging ends within the simulation period is reported. As expected, Table 3 shows that the uncontrolled case would allow all PEVs to be charged with a minimum time (20.31 min).

It is important to remark that this charging time corresponds to a desired SoC value of 0.9, whereas the SoC of 0.8 is reached in about ten minutes. This is consistent with the definition of UFC [27].

**Table 2.** Arrival time of the PEVs.

Charging Station		Arrival Time (hh:Min)	Arrival Time (hh:Min)
CS <sub>1</sub>	Pos. 1	11:03	11:29
	Pos. 2	11:03	11:29
	Pos. 3	11:05	11:31
	Pos. 4	11:04	11:30
CS <sub>2</sub>	Pos. 1	11:03	11:29
	Pos. 2	11:00	11:26
	Pos. 3	11:02	11:28
	Pos. 4	11:02	11:28
CS <sub>3</sub>	Pos. 1	11:03	11:29
	Pos. 2	11:00	11:26
	Pos. 3	11:03	11:29
	Pos. 4	11:02	11:28
CS <sub>4</sub>	Pos. 1	11:00	11:26
	Pos. 2	11:00	11:26
	Pos. 3	11:02	11:28
	Pos. 4	11:02	11:28

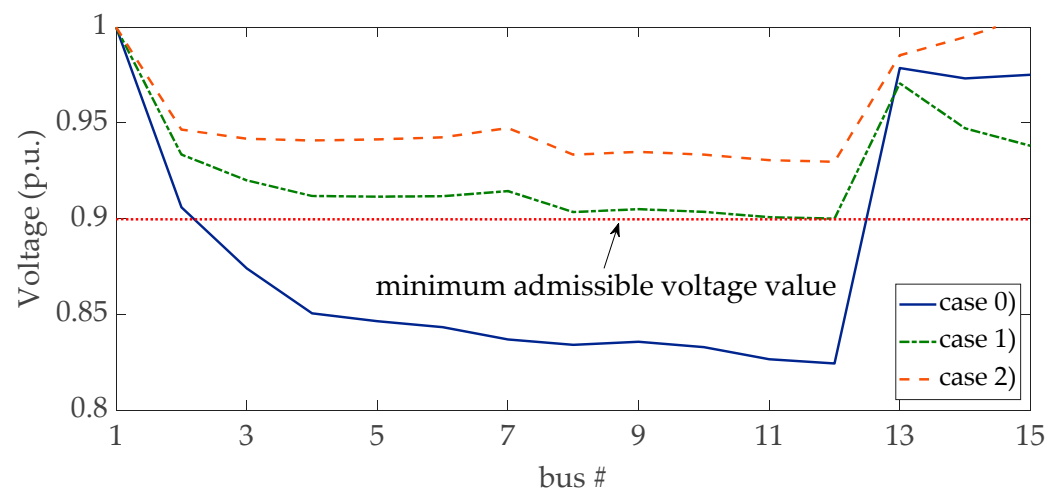
**Table 3.** Charging time of the PEVs.

Charging Station		Arrival Time (hh:Min)	Charging Time [Min]		
			Uncontrolled Case (0)	Controlled Case (1)	Controlled Case (2)
CS <sub>1</sub>	Pos. 1	11:03	20.31	20.32	20.31
	Pos. 2	11:03	20.31	20.32	20.31
	Pos. 3	11:05	20.31	20.81	24.88
	Pos. 4	11:04	20.31	20.32	20.31
CS <sub>2</sub>	Pos. 1	11:03	20.31	20.31	22.29
	Pos. 2	11:00	20.31	20.31	21.43
	Pos. 3	11:02	20.31	20.31	21.29
	Pos. 4	11:02	20.31	20.31	21.29
CS <sub>3</sub>	Pos. 1	11:03	20.31	20.67	21.71
	Pos. 2	11:00	20.31	20.54	21.49
	Pos. 3	11:03	20.31	20.67	21.71
	Pos. 4	11:02	20.31	20.54	21.25
CS <sub>4</sub>	Pos. 1	11:00	20.31	20.31	21.17
	Pos. 2	11:00	20.31	20.31	21.17
	Pos. 3	11:02	20.31	20.31	21.17
	Pos. 4	11:02	20.31	20.31	21.17

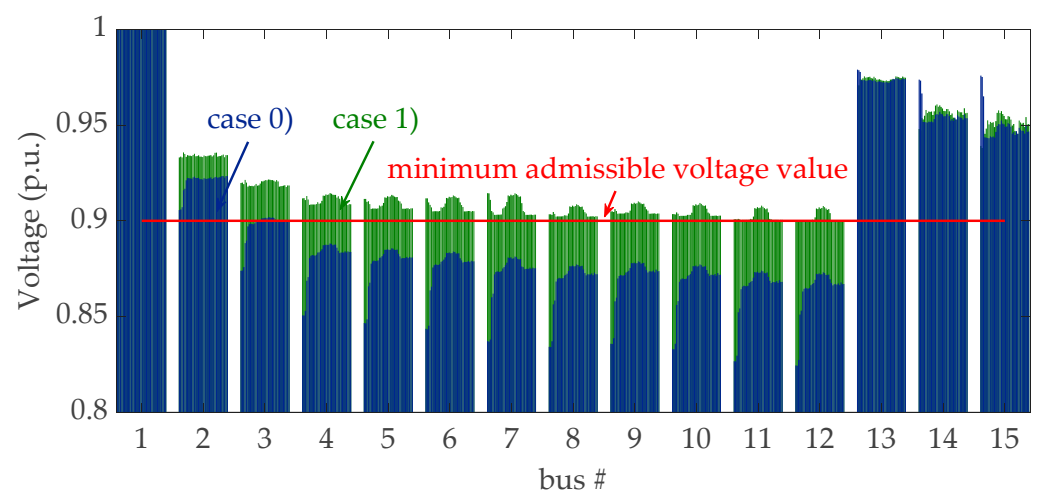
As a measure of the impact of the proposed approach, it is important to compare the overall charging time of the PEVs that during the simulation period reach a SoC of 0.9. In *case (0)* (uncontrolled), the overall charging time is 324.96 min, its value in *case (1)* is 326.66 min and it is 336.82 min in *case (2)*, all referring to the same number of fully charged PEVs (16). These results clearly show that, thanks to the control of the active and reactive powers of the UFC stations and of the reactive power of the PV systems, the proposed approach allows satisfaction of the technical constraints on the network with only a slight delay on the charging time (326.66 min in *case (1)* instead of 324.96 min in the uncontrolled case). This delay increases in case of larger support requested of the reactive power from

the UFC station. Moreover, further simulations were performed by considering the PEVs fully charged at 0.8 SoC, which showed even lower differences between the charging times observed in the controlled and uncontrolled cases. With reference to the UFC station located at bus #15, no differences appear among the charging times of *case (0)* and *case (1)*. This is due to the proximity of the PV system to the UFC station. This condition has no effect in *case (2)* due to the stringent constraints on the power factor at the PCC.

Regarding the microgrid technical constraints, it is worth noting that the uncontrolled case implies unfeasible grid operation in terms of allowable bus voltage. As an example, in Figure 8a the bus voltage profile at 11.02 a.m. is reported, in which the voltage reaches its minimum value; in the figure, the voltage profiles corresponding to the three case studies are shown. In Figure 8b the bus voltage values at each time interval are shown. For the sake of clarity, only the results corresponding to *case (0)* and *case (1)* are reported.



(a)



(b)

**Figure 8.** Voltage profile corresponding to the three case studies (hour 11:02) (a); bus voltage values at all time intervals corresponding to *case (0)* and *case (1)* (b).

As clearly depicted in Figure 8, the minimum admissible voltage level is exceeded in the case of uncontrolled case (*case (0)*). In *case (1)*, the control of the PEVs' charging power and the support of reactive power from the DG units and UFC stations, allows the obtaining of a voltage profile which satisfies the admissible limits. Obviously, this implies a reduction of the charging power of some of the PEVs, so resulting in a slight increment

of the charging time. In *case (2)*, the constraint imposed on the power factor at the PCC implies an increased reactive power provision from the UFC stations and DG units. This results in a higher voltage profile and a reduced active power available for PEVs' charging, so leading to an increased value of the charging time.

The power profile of the UFC station at bus #12 (UFCS<sub>3</sub>) is reported in Figure 9 with respect to the three case studies.

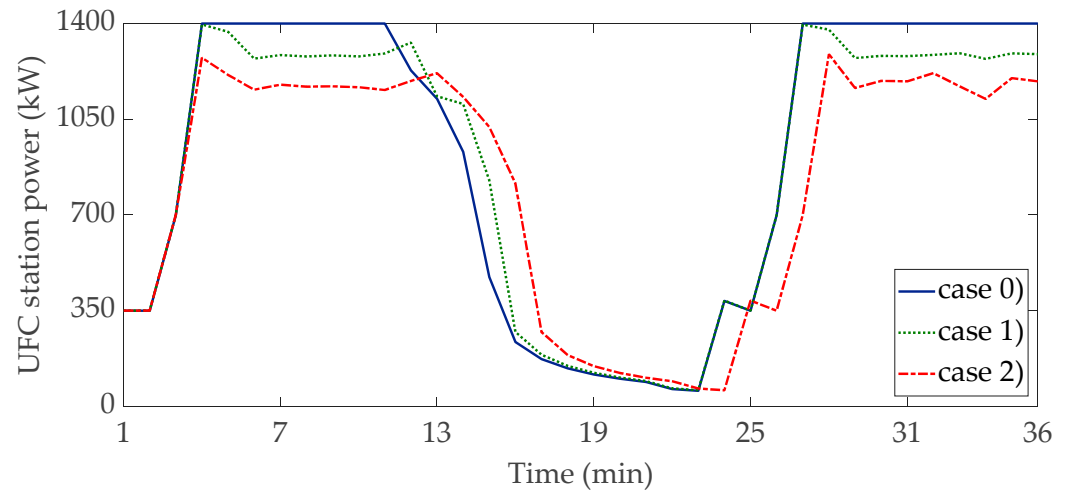


**Figure 9.** Power profile of the UFC station at bus #12 (UFCS<sub>3</sub>) in the three case studies.

Compared to the ideal case (*case (0)*), the reduction of the power absorbed from the microgrid in the *cases (1)* and *(2)* clearly appears. In *case (2)*, the reduction of the absorbed power is greater than that in *case (1)*. In agreement with the results of Table 3, the longer charging time of *case (2)* is more apparent and can be well appreciated in Figure 9, and the smaller difference in the charging times of *cases (0)* and *(1)* is also clear.

In Figure 10 the powers absorbed by all PEVs plugged-in at the UFCS<sub>3</sub> during the considered period are reported with respect to the three case studies. The corresponding SoC profiles are reported in Figure 11. By comparing the profiles of *case (1)* and *(2)* with those of *case (0)*, in Figures 10 and 11, the ability of the proposed approach to properly manage the power of the vehicles to meet the vehicle constraints is evident.

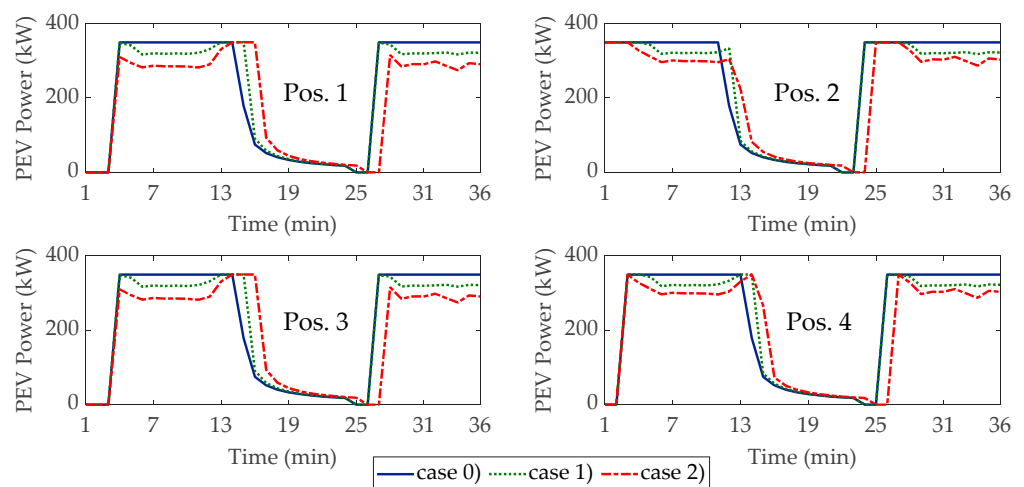


**Figure 10.** Power profile of the PEVs plugged-in the UFC station at bus #12 (UFCS<sub>3</sub>) in the three case studies.

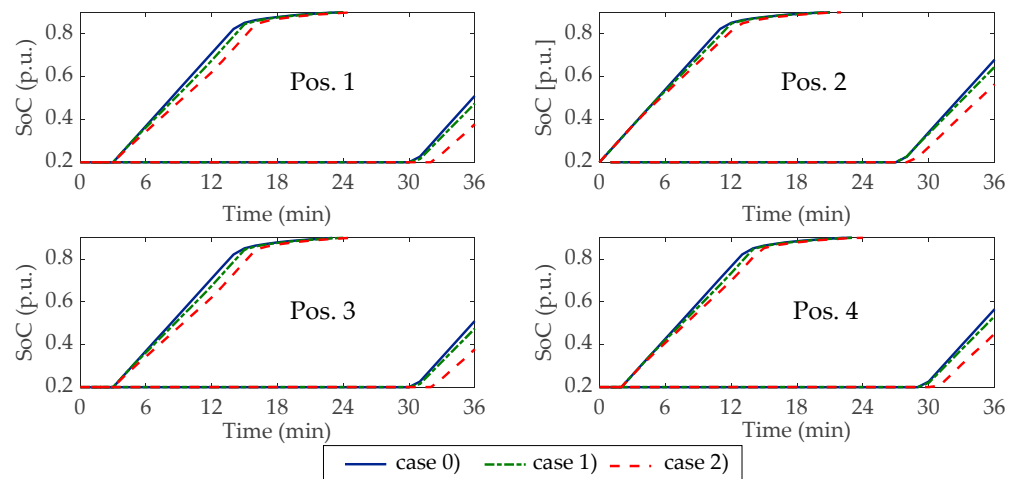


**Figure 11.** SoC profile of the PEVs plugged-in the UFC station at bus #12 (UFCS<sub>3</sub>) in the three case studies.

Compared to *case (1)*, the increased power reduction in *case (2)* depends on the increased reactive power support requested from the UFC stations. In Figure 12, the reactive power provided by the UFCS<sub>3</sub> is reported with respect to *case (1)* and *case (2)* (obviously, there is no reactive support from the UFC stations in the uncontrolled case).

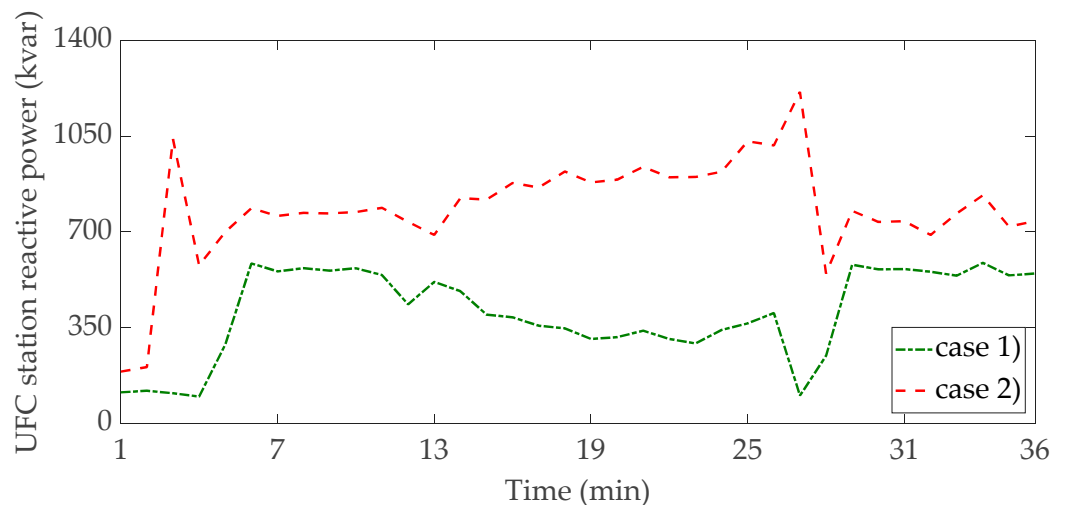


**Figure 12.** Reactive power profile of the UFCS<sub>3</sub> located at bus #12 in the three case studies.

Figure 13 reports the reactive power provided by the PV system connected to the bus #15. In this case, the increased contribution of reactive power to satisfy the constraint on the power factor (0.9) imposed at the PCC is also apparent. The results in terms of the power factor during the considered power profile is reported in Figure 14, in the *cases (1)* and *(2)*, where the satisfaction of the minimum power factor is clearly apparent.

Further simulations were performed in which the initial SoC of the vehicles is assumed to vary according to a uniform distribution in the range (20%, 70%). In addition, to consider different operating conditions, two scenarios have been analyzed which refer to the arrival time of each vehicle supposed to uniformly vary within 5 (Scenario A) and 10 (Scenario B) minutes. The results are reported in Table 4. For comparative purposes, the same number of vehicles have been supposed for the scenarios A and B, each having the same state of charge at the arrival identified through the aforementioned uniform distribution.

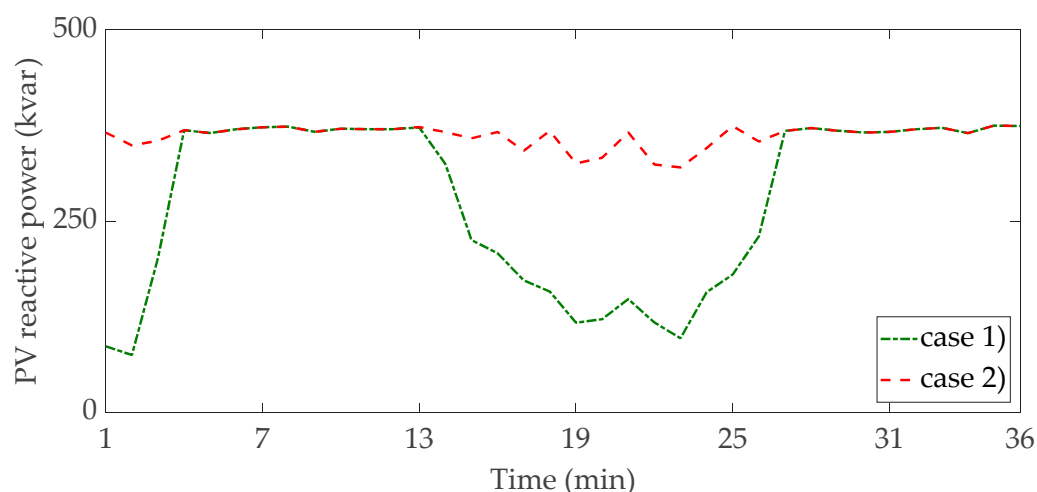


Figure 13. Reactive power profile of the PV located at bus #15 in the three case studies.

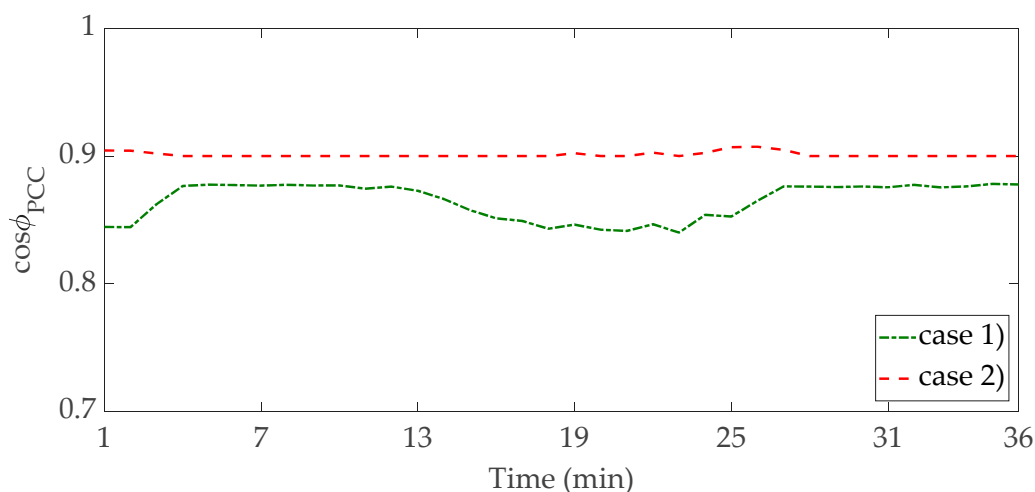


Figure 14. Power factor at the PCC.

Table 4. Charging time of the PEVs for different arrival time scenarios.

	Charging Time of PEVs (Min)		
	Uncontrolled Case (0)	Controlled Case (1)	Controlled Case (2)
Scenario A	267.05	267.84	273.57
Scenario B	267.05	267.06	270.52

The results reported in Table 4 clearly show that in the case of weak charging demand (Scenario B) the proposed approach appears effective, even if the difference with the uncontrolled case is clearly smaller. The lower values of the results compared to those reported above are due to the different values of the charging time which depend on the state of charge at the arrival time (in the original case studies vehicles are all supposed to arrive at 20% SoC). Moreover, it can be noted that, when more vehicles are charging contemporaneously (i.e., in the case of Scenario A), longer time is required to charge the vehicles compared to the case of Scenario B. This is due to the need to satisfy the microgrid technical constraints in more critical operating conditions (i.e., higher load demand). In case (2) even longer charging time is required compared to the other cases due to the even more stringent constraints assumed in this case study.

#### 4. Conclusions

In this paper a methodology is discussed which allows managing the ultra-fast charge of fleets of plug-in electric vehicles in microgrids. The proposed methodology makes it possible to meet the desired reduction of charging time with the impact of ultra-fast charging infrastructure in the distribution networks. The increased performances of ultra-fast infrastructures, indeed, make even more complex the management of power supply at distribution level with particular emphasis to the effects produced on the bus voltages and line currents. The proposed approach uses the ability of the ultra-fast charging equipment to control the active charging power and the reactive power exchanged with the grid. In more detail, by controlling active and reactive powers of the converter interface used to connect the charging station to the microgrid, it is demonstrated that it is possible to get both the expected reduced charging time and the microgrids' operational constraints. Even in the case of large penetration of ultra-fast charging infrastructures, this can be achieved by optimally coordinating in real-time the microgrid resources with a negligible increase of charging time. The results of the numerical applications also demonstrate that the effect of charging time can be slightly increased when an increased support in terms of reactive power is requested of the microgrids' resources. To consider also the economic aspects related to the use of ultrafast charging stations, future works will focus on the optimal planning of the charging stations controlled through the approach proposed in this paper.

**Author Contributions:** Conceptualization, D.P., L.P.d.N., F.M. and R.R.; methodology, D.P. and F.M.; software, D.P. and F.M.; validation, D.P., F.M., L.P.d.N. and R.R.; writing—original draft preparation, D.P. and F.M.; writing—review and editing, D.P., F.M., L.P.d.N. and R.R. All authors have read and agreed to the published version of the manuscript.

**Funding:** This research received no external funding.

**Institutional Review Board Statement:** Not applicable.

**Informed Consent Statement:** Not applicable.

**Data Availability Statement:** Not applicable.

**Conflicts of Interest:** The authors declare no conflict of interest.

#### Nomenclature

DG	distributed generation
$E_{pev,i,j}^n$	on-board battery capacity of the PEV connected to the $i$ th charger of the $j$ th charging station
OPF	optimal power flow
$P_{pev,i,j,k}$	charging power of the $i$ th charger of the $j$ th charging station at the time interval $k$
$P_{pev,i,j}^n$	power rating of the $i$ th charger of the $j$ th charging station
$p_{SoC,i,j,k}^{max}$	the maximum charging power of the on-board battery connected to the $i$ th charger of the $j$ th charging station at the time interval $k$
$P_{SoC,i,j,k}^n$	power rating of the onboard battery
PCC	point of common coupling
PEV	plug-in electric vehicles
PV	photovoltaic
SoC	state of charge
$SoC_{dp,i,j}$	desired value of the battery SoC of the $i$ th PEV connected to the $j$ th charging station
$SoC_{i,j,k-1}$	value of the battery SoC of the $i$ th PEV connected to the $j$ th charging station at the beginning of the $k$ th time interval
$SoC_{i,j,0}$	specified input value of SoC at the beginning of the charging stage of each PEV
UFC	ultra-fast charging
$n_{pev,j,k}$	number of PEVs connected at the $j$ th charger at the time interval $k$
$n_{cs}$	number of charging stations connected to the microgrid
$\eta_{pev,j}$	efficiency of the chargers located at the $j$ th charging station
$\lambda_{i,j}$	decay constant

## References

1. Srdic, S.; Liang, X.; Zhang, C.; Yu, W.; Lukic, S. A SiC-based high-performance medium-voltage fast charger for plug-in electric vehicles. In Proceedings of the IEEE Energy conversion congress and exposition (ECCE), Milwaukee, WI, USA, 18–22 September 2016.
2. Leone, C.; Longo, M. Modular Approach to Ultra-fast Charging Stations. *J. Electr. Eng. Technol.* **2021**, *16*, 1971–1984. [CrossRef]
3. Tahir, Y.; Khan, I.; Rahman, S.; Nadeem, M.F.; Iqbal, A.; Xu, Y.; Rafi, M. A state-of-the-art review on topologies and control techniques of solid-state transformers for electric vehicle extreme fast charging. *IET Power Electron.* **2021**, *14*, 1560–1576. [CrossRef]
4. Brenna, M.; Foadelli, F.; Leone, C.; Longo, M. Electric Vehicles Charging Technology Review and Optimal Size Estimation. *J. Electr. Eng. Technol.* **2020**, *15*, 2539–2552. [CrossRef]
5. Ronanki, D.; Kelkar, A.; Williamson, S.S. Extreme Fast Charging Technology—Prospects to Enhance Sustainable Electric Transportation. *Energies* **2019**, *12*, 3721. [CrossRef]
6. Fastned. Superfast Charging. Available online: <https://support.fastned.nl/hc/en-gb> (accessed on 5 November 2021).
7. Ayoub, E.; Karami, N. Review on the charging techniques of a Li-Ion battery. In Proceedings of the Third International Conference on Technological Advances in Electrical, Electronics and Computer Engineering (TAEECE), Beirut, Lebanon, 29 April–1 May 2015; pp. 50–55.
8. Solanke, T.U.; Khatua, P.K.; Ramchandaramurthy, V.K.; Yong, J.Y.; Tan, K.M. Control and management of a multilevel electric vehicles infrastructure integrated with distributed resources: A comprehensive review. *Renew. Sustain. Energy Rev.* **2021**, *144*, 111020. [CrossRef]
9. Amin, A.; Tareen, W.U.K.; Usman, M.; Ali, H.; Bari, I.; Horan, B.; Mekhilef, S.; Asif, M.; Ahmed, S.; Mahmood, A. A Review of Optimal Charging Strategy for Electric Vehicles under Dynamic Pricing Schemes in the Distribution Charging Network. *Sustainability* **2020**, *12*, 10160. [CrossRef]
10. Huajie, D.; Zechun, H.; Yonghua, S.; Xiaorui, H.; Yongxiang, L. Coordinated control strategy of energy storage system with electric vehicle charging station. In Proceedings of the IEEE Conference and Expo Transportation Electrification Asia-Pacific (ITEC Asia-Pacific), Beijing, China, 31 August–3 September 2014.
11. Bitencourt, L.d.A.; Borba, B.S.; Maciel, R.S.; Fortes, M.Z.; Ferreira, V.H. Optimal EV charging and discharging control considering dynamic pricing. In Proceedings of the 2017 IEEE Manchester PowerTech, Manchester, UK, 18–22 June 2017; pp. 1–6.
12. Anderson, E. Real-time pricing for charging electric vehicles. *Electr. J.* **2014**, *27*, 105–111. [CrossRef]
13. Masoum, A.S.; Deilami, S.; Moses, P.S.; Masoum, M.A.; Abu-Siada, A. Smart load management of plug-in electric vehicles in distribution and residential networks with charging stations for peak shaving and loss minimisation considering voltage regulation. *IET Gener. Transm. Distrib.* **2011**, *5*, 877–888. [CrossRef]
14. Deilami, S.; Masoum, A.S.; Moses, P.S.; Masoum, M.A. Real-time coordination of plug-in electric vehicle charging in smart grids to minimize power losses and improve voltage profile. *IEEE Trans. Smart Grid* **2011**, *2*, 456–467. [CrossRef]
15. Hajforoosh, S.; Masoum, M.A.; Islam, S.M. Online optimal variable charge-rate coordination of plug-in electric vehicles to maximize customer satisfaction and improve grid performance. *Electr. Power Syst. Res.* **2016**, *141*, 407–420. [CrossRef]
16. Tareen, W.U.K.; Mekhilef, S.; Nakaoka, M. A transformerless reduced switch counts three-phase APF-assisted smart EV charger. In Proceedings of the 2017 IEEE Applied Power Electronics Conference and Exposition (APEC), Tampa, FL, USA, 26–30 March 2017; pp. 3307–3312.
17. Binetti, G.; Davoudi, A.; Naso, D.; Turchiano, B.; Lewis, F.L. Scalable real-time electric vehicles charging with discrete charging rates. *IEEE Trans. Smart Grid* **2015**, *6*, 2211–2220. [CrossRef]
18. Kongjeen, Y.; Bhumkittipich, K. Impact of Plug-in Electric Vehicles Integrated into Power Distribution System Based on Voltage-Dependent Power Flow Analysis. *Energies* **2018**, *11*, 1571. [CrossRef]
19. Jovanovic, R.; Bayhan, S.; Bayram, I.S. An Online Model for Scheduling Electric Vehicle Charging at Park-and-Ride Facilities for Flattening Solar Duck Curves. In Proceedings of the International Joint Conference on Neural Networks (IJCNN), Glasgow, UK, 19–24 July 2020; pp. 1–8.
20. Höimoja, H.; Vasiladiotis, M.; Grioni, S.; Capezzali, M.; Rufer, A.; Püttgen, H.B. Toward Ultrafast Charging Solutions of Electric Vehicles. In Proceedings of the 2012 CIGRE Session, Paris, France, 26–31 August 2012.
21. Mandrile, F.; Cittanti, D.; Mallemaci, V.; Bojoi, R. Electric Vehicle Ultra-Fast Battery Chargers: A Boost for Power System Stability? *World Electr. Veh. J.* **2021**, *12*, 16. [CrossRef]
22. Srdic, S.; Lukic, S. Toward Extreme Fast Charging: Challenges and Opportunities in Directly Connecting to Medium-Voltage Line. *IEEE Electr. Mag.* **2019**, *7*, 22–31. [CrossRef]
23. Dixon, J.; Andersen, P.B.; Bell, K.; Træholt, C. On the ease of being green: An investigation of the inconvenience of electric vehicle charging. *Appl. Energy* **2020**, *258*, 114090. [CrossRef]
24. Benchmark Systems for Network Integration of Renewable and Distributed Energy Resources, Cigré Task Force C6.04, Cigré Brochure 575, April 2014. Available online: [https://e-cigre.org/publication/ELT\\_273\\_8-benchmark-systems-for-network-integration-of-renewable-and-distributed-energy-resourcesets](https://e-cigre.org/publication/ELT_273_8-benchmark-systems-for-network-integration-of-renewable-and-distributed-energy-resourcesets) (accessed on 21 January 2022).
25. IEEE Open Data Sets. Available online: <http://site.ieee.org/pes-iss/data-sets> (accessed on 21 January 2022).

- 
26. Suarez, C.; Martinez, W. Fast and Ultra-Fast Charging for Battery Electric Vehicles—A Review. In Proceedings of the 2019 IEEE Energy Conversion Congress and Exposition (ECCE), Baltimore, MD, USA, 29 September–3 October 2019; pp. 569–575.
  27. Leong, C.K.; Gan, Y.H.; Gan, G.D.; Phuan, Z.Y.; Yoong, M.K.; Cheah, B.K.; Chew, K.W. Ultra fast charging system on lithium ion battery. In Proceedings of the 2010 IEEE Conference on Sustainable Utilization and Development in Engineering and Technology, Kuala Lumpur, Malaysia, 20–21 November 2010; pp. 37–39.